Veterinary Surgery
38:161–168, 2009

Visual Estimation of Radioulnar Incongruence in Dogs Using Three-Dimensional Image Rendering: An In Vitro Study Based on Computed Tomographic Imaging

PETER BÖTTCHER, Dr Med Vet, Diplomate ECVS, HINNERK WERNER, DVM, EBERHARD LUDEWIG, Dr Med Vet, Diplomate ECVDI, VERA GREVEL, Prof Dr Med Vet, Diplomate ECVS, and GERHARD OECHTERING, Prof Dr Med Vet, Diplomate ECVAA

Objective—To determine the sensitivity and specificity of visual estimation of radioulnar incongruence (RUI) in the canine elbow by use of 3-dimensional (3D) image rendering.
Study Design—Experimentally induced negative and positive RUI.
Sample Population—Canine (>20 kg) cadaveric right thoracic limbs (n = 8).
Methods—Radial shortening and lengthening of 1 and 2 mm were performed extending an established surgical in vitro model of RUI. Based on transverse computed tomographic (CT) scans of each radioulnar conformation, the subchondral radioulnar joint surface was reconstructed and visualized. A total of 64 3D models of RUI were blindly evaluated in a random manner by 3 independent observers. RUI was estimated subjectively at 1 mm precisely (−2, −1, 0, +1, +2) by visual inspection of the 3D models.
Results—Median sensitivity for identifying an incongruent joint was 0.86. Median specificity for identification of a congruent joint was 0.77. Analyzing the data only in respect to a congruent joint versus one with a shortened radius (positive RUI) resulted in a median sensitivity of 0.82, and a median specificity of 1.00. Interobserver agreement was 0.87. Repeatability was 0.96.
Conclusion—Estimation of positive and negative RUI based on 3D surface models of the radioulnar articulation mimics gross inspection in a noninvasive manner, the latter being the ultimate gold standard for definitive diagnosis of any radioulnar step. The proposed technique is precise, reliable, and repeatable in vitro.
Clinical Relevance—Preoperative estimation of the type and degree of RUI is the basis for deciding which type of corrective or modifying osteotomy might be best suited to restore normal joint loads in vivo.

INTRODUCTION

THE CAUSE and pathogenesis of fragmented medial coronoid process (MCP), osteochondrosis of the humeral trochlea as well as their advanced stages in the form of medial compartment disease with complete loss of hyaline cartilage are poorly understood. Traditionally, mechanical overloading because of joint incongruence has been proposed as the most probable underlying cause.[1,2] Fatigue microdamage in the region of the MCP has been documented even in the absence of obvious cartilage degeneration,[3] strengthening the hypothesis of chronic supraphysiologic loading of the medial compartment in dysplastic elbows.

Proposed types of joint incongruence are mismatching of the trochlear notch of the ulna and the humeral condyle as well as a positive step forming at the level of the transition of the ulnar and radial joint surface.[4–8]

From the Department of Small Animal Medicine, University of Leipzig, Leipzig, Germany.
Presented in part at the ACVS Annual Scientific Meeting, Chicago, IL, October 18–21, 2007.
Address reprint requests to Dr. Peter Böttcher, Diplomate ECVS, Klinik für Kleintiere, An den Tierkliniken 23, D-04103 Leipzig, Germany. E-mail: boettcher@kleintierklinik.uni-leipzig.de.
Submitted April 2008; Accepted September 2008

0161-3499/09
doi:10.1111/j.1532-950X.2008.00483.x

The latter has been advocated as the most important factor and has become the traditional model of elbow incongruence, in which a shortened radius results in increased mechanical pressure on the MCP and humeral trochlea, as joint compression forces are no longer evenly distributed between the radial and ulnar joint surfaces.[8] Even though this model might explain most of the pathology encountered in the medial compartment of dysplastic canine elbows, the coexistence of an un-united anconeal process (UAP) with an obviously shortened ulna and fragmented MCP in the same joint seems illogical.[9] Mismatch of the trochlear notch can also hardly explain the low incidence of both fragmented MCP and UAP in the same joint.[5]

Based on these obvious limitations of the traditional model of elbow incongruence, a more advanced model has been proposed.[10] The so-called "Angular Vector Model" considers negative as well as positive radioulnar incongruence (RUI) as the major factors leading to physical overloading of the medial joint compartment. Based on this, the simplification of RUI to a shortened radius (positive RUI) only, seems questionable.[11–13] The same rationale would hold for any corrective or modifying osteotomy when approaching the dysplastic elbow.[8,14–18]

When performing as well as evaluating such invasive procedures exact preoperative as well as postoperative estimation of RUI seems imperative. Radiographic evaluation of positive RUI has poor sensitivity and specificity.[12] Computed tomography (CT) scores far better and is considered the gold standard in clinical practice.[11,19–21] Recently, arthroscopic evaluation of positive RUI has been reported to be of superior accuracy in vitro compared with all diagnostic imaging modalities evaluated to date.[13]

Struggling with the precise, noninvasive quantification of suspected RUI, we investigated whether the extension of 2-dimensional (2D) CT measurement in the form of 3-dimensional (3D) models of the subchondral radioulnar joint surface may increase accuracy. We also investigated positive and negative RUI to account for the more complex understanding of elbow incongruence.[10]

MATERIALS AND METHODS

Specimens

Right thoracic limbs of 8 mature, middle to large breed dogs (weighing >20 kg) with no history of lameness for the harvested limb were collected after euthanasia of the dogs for reasons unrelated to this study. Elbow joint pathology was excluded based on complete radiographic and CT examination, and later confirmed by elbow joint disarticulation and inspection of the joint surfaces for visible cartilage damage.

Experimental Model of RUI

RUI was experimentally induced using an in vitro model.[11,12] Briefly, a 4-pin type 1 unilateral external skeletal fixator was applied to the cranial aspect of the radial diaphysis (Fig 1). The 4 fixation pins were connected to a custom made linear sidebar allowing both lengthening and shortening with micromillimeter accuracy. Axial stability of the sidebar as well as bending properties had been tested using a material-testing machine to 1000 N. A 3.5 mm cortical screw was inserted from the lateral to the medial styloid process to eliminate any axial movement between the distal radius and the ulna. The interosseous ligament was cut allowing unconstrained movement of the proximal radius in relation to the ulna. The radius was osteotomized midway between the 2 central fixator pins, removing a bone block of ~ 1 cm length. In extension of the established model,[11,12] shortening as well as lengthening of the radius was performed at 1 mm increments from 0 to 2 mm.

3D Evaluation of RUI

Within each of the 8 elbow joints, 8 states of RUI were evaluated: 4 incongruent (-2, -1, $+1$, $+2$ mm), 1 congruent (0 mm) state of the radioulnar junction, and 3 randomly chosen repetitions (from -2 over 0 to $+2$ mm). The sequence for creating RUI states was also randomly defined. Randomizations were performed using a freely available random list generator (http://www.random.org/).

Each time the linear sidebar was lengthened or shortened, a complete transverse CT scan of the elbow joint was performed simulating sternal recumbency with the elbow joint at an angle of $\sim 135°$. Acquisition of CT data was performed on a multislice helical CT-scanner (Philips Brilliance, Philips, Eindhoven, the Netherlands) with an average in-plane resolution of 0.159 mm (SD = 0.011 mm) and a slice thickness of

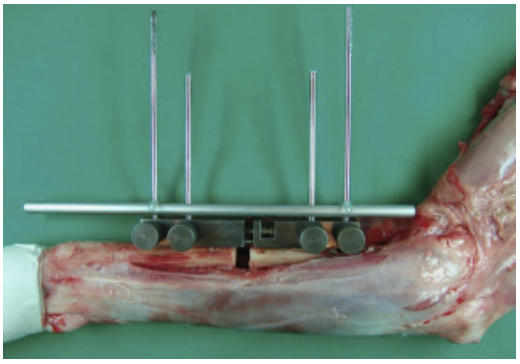

Fig 1. Experimental setup of the in vitro model for precise creation of positive as well as negative radioulnar incongruence (RUI) at the level of the elbow joint. The radius has been osteotomized and rigidly reconstructed using a type 1 unilateral external skeletal fixator connected with a linear sidebar. The aluminum rod, which extends up to the level of the humeral epicondyles, defines the axis of lengthening and shortening exerted by the linear sidebar, visible in each transverse computed tomographic (CT) scan of the elbow joint.

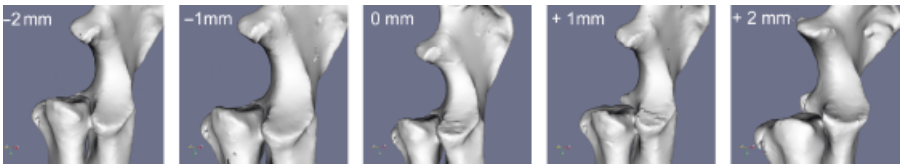

Fig 2. Three-dimensional (3D) models of the 5 simulated radioulnar conformations.

1 mm with an overlapping increment of 0.5 mm. Image reconstruction was done using a sharp bone filter (FilterType and ConvolutionKernel D; Philips).

After data acquisition, 3D surface models of the elbow joint were calculated using dedicated image analysis software based on the Visualization ToolKit,[22] (Kitware Inc., New York, NY, USA) an open source, freely available software system for 3D computer graphics, image processing, and visualization. Further enhancement as well as inspection of the 3D models were performed using ParaView (Kitware Inc., New York, NY, USA) (http://www.paraview.org/New/index.html) an open-source, multiplatform visualization framework.

As the radioulnar joint surfaces are hidden by the distal humerus, we had to simulate artificial disarticulation of the reconstructed elbow joint to get isolated 3D models of the proximal radius and ulna (Fig 2). The humerus was manually delineated within the original image slices. Using that extracted humerus as a template it was rigidly matched onto the other CT volumes of the same elbow using custom made image registration software.[23] Deleting the matched template from each image volume allowed computation of an isolated 3D model of radius and ulna.

Finally, the 64 3D models were randomized and blindly evaluated by 3 independent investigators (E.L., P.B., H.W.). Using the ParaView visualization framework, each investigator was free to inspect each 3D model at his own pace by moving, scaling, and rotating the model on the computer screen. In the end, each observer had to estimate the RUI present at 1 mm precisely, with an RUI of zero representing a congruent joint.

Evaluation of the Experimental Model of RUI

First, we determined that application of the sidebar with osteotomy of the radius did not induce RUI compared with the native elbow. Therefore, 3 transverse CT data sets, referred to as A1–A3, were acquired before RUI investigation. The 1st scan was of the native elbow (A1), the 2nd after osteotomy of the radius and application of the linear sidebar (A2), and the 3rd after several evenly chosen cycles of lengthening and shortening of the radius (A3). Before CT scanning of A2 and A3 as well as for the 8 induced RUI states, an aluminum rod extending up to the level of the humeral epicondyles was rigidly connected to the linear sidebar (Fig 1).

Because the rod was fixed parallel to the long axis of the sidebar, its long axis within the image volume represented precisely the axis along the experimentally induced lengthening and shortening of the radius. As the native elbow (A1) had no sidebar attached and therefore no reference rod could be attached to it, the image data of the reference tube of A2 were transformed into A1. This was done based on the transformation matrix obtained after matching the manually extracted radius of A2 onto A1, similar to that described for the humerus. This step equipped the native elbow data with a reference for the axis of future lengthening and shortening exerted onto the radius in the subsequent image volumes.

As already described for the 8 states of RUI, A1–A3 were then processed similarly resulting in a 3D model of the proximal radius and ulna together with the 3D model of the reference rod. After removal of the humerus and automatic calculation of the long axis of the reference rod using oriented bounding box tree calculation,[24] the distance of the most proximal points of the radius and the ulna parallel to the long-axis of the reference rod was measured within the 3 3D models (A1–A3; Fig 3). Pairwise comparison using the Wilcoxon signed ranks test between the value measured on A1 and the values obtained on A2 and A3, respectively, allowed

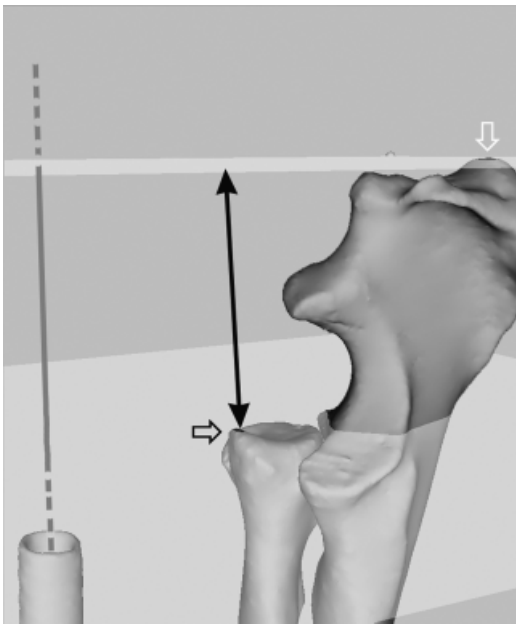

Fig 3. Measurement of relative position of the radius with respect to the ulna. Two parallel planes (white) orthogonal to the long axis (gray dotted line) of the 3-dimensional (3D) model of the aluminum rod were manually positioned, 1 at the most proximal point of the radius (black open arrow) and 1 at the most proximal point of the ulna (white open arrow). The distance of those 2 planes (black short arrow) measured perpendicular to the long axis of the aluminum rod (gray dotted line) defined the proximodistal position of the radius relative to the ulna.

estimation of inadvertently induced RUI attributed to the experimental setup. A P-value $< .05$ was considered significant.

Corresponding to that, the effective amount of RUI induced by lengthening and shortening of the linear sidebar had to be evaluated for the 8 RUI states investigated. Therefore, the distance of the most proximal point of radius and ulna in the subsequent 3D models of experimentally induced RUI was measured as described for A1–A3. Subtracting that value from the one measured on A1 gave the relative movement of the proximal radius in relation to the proximal ulna. Pearson product moment correlation coefficients analysis of that value and the presumed RUI induced on the linear sidebar gave an estimate of model accuracy.

Data Analysis

Statistical calculations were performed using the software SPPS 13.0 for Windows (SPSS Inc., Chicago, IL). Sensitivity and specificity were calculated based on crosstable calculation for each investigator separately. The overall sensitivity and specificity were expressed as the median of the 3 investigators. Three different definitions of RUI were investigated: (1) estimation of an incongruent versus a congruent joint, summarizing all states of RUI different from a congruent joint, with respect to the "Angular Vector Model," (2) all positive RUIs versus the congruent joint reflecting the shortened radius scenario of the traditional model of RUI, and (3) all negative RUIs versus the congruent joint. As the study design used 2 possible states of incongruence, underestimation of specificity would be inevitable when applying the traditional definition of a congruent joint as "the unmodified elbow,"[13] Therefore, congruence was defined in (2) and (3) as any state different from the one analyzed when calculating sensitivity.

Finally, we analyzed our data only with respect to severe RUI (≥ 2 mm). Therefore, sensitivity for an RUI of -2 or $+2$ mm was calculated with respect to whether the joint was scored as incongruent, either as a $-2/+2$ mm RUI or as a $-1/+1$ mm RUI.

The intraclass correlation coefficient (ICC) was used to quantify inter- as well as intraobserver variability. Intraobserver repeatability was determined with correlations between measurements by 1 randomly chosen individual (H.W.), estimating RUI on the 64 3D models 3 times at a weekly interval. Interobserver repeatability was determined with correlations between estimations of the 3 individuals.

RESULTS

Reliability of the Experimental Model of RUI

No significant changes in relative radioulnar position were introduced during the experimental setup ($P = .375$). Even after several cycles of lengthening and shortening the native state of the radioulnar transition was re-established ($P = .078$).

Comparing relative movement of the proximal radius of the 8 RUI states with respect to the native unchanged elbow (A1) and the presumed proximodistal movement of the radius exerted by the sidebar had a correlation coefficient (R-value) of 0.996 ($R^2 = 0.992$; Fig 4).

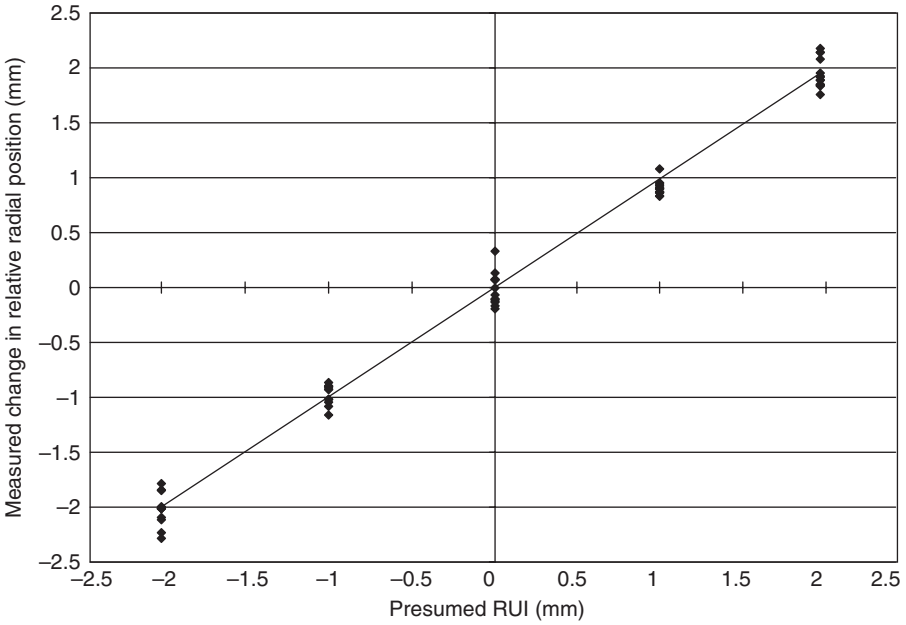

Fig 4. Pearson correlation between presumed radioulnar incongruence (RUI) and the change in relative position of the radius measured within the 3-dimensional (3D) models of the 8 RUI states investigated within each elbow with respect to the native, unchanged elbow A1 (R-value of 0.996 [$R^2 = 0.992$]).

Table 1. Cross-Table Summarizing Results for 3 Investigators for 64 Models of Radioulnar Incongruence (RUI) (n = 64)

	−2 mm RUI	−1 mm RUI	0 mm RUI	+1 mm RUI	+2 mm RUI	Estimated Incidence
Estimated RUI −2 mm	5–9–5	3–3–0				8–12–5
Estimated RUI −1 mm	6–2–6	8–7–12	5–1–1			19–10–19
Estimated RUI 0 mm		1–2–0	8–10–12	6–5–1	2–0–0	17–17–13
Estimated RUI +1 mm			0–2–0	7–7–13	6–9–1	13–18–14
Estimated RUI +2 mm				1–2–0	6–5–13	7–7–13
True incidence	11	12	13	14	14	

The results for the 3 investigators are listed separated by a dash: investigator 1–investigator 2–investigator 3. The lower line summarizes the true incidence of each state of RUI within the 64 models investigated. The row on the right summarizes the number of estimations of each investigator for the 5 possible states of RUI.

Sensitivity and Specificity (Tables 1 and 2)

Randomization of 3 additional RUI states resulted in an even distribution of each simulated RUI. The frequency of each RUI within the 64 3D models investigated was as follows: −2 mm RUI = 11 times, −1 mm RUI = 12, a congruent radioulnar joint = 13, +1 mm RUI = 14, and +2 mm RUI = 14. Ratings of the 64 models by the 3 investigators separately are summarized (Table 1).

Median sensitivity for detecting any form of incongruent joint was 0.86 (range, 0.82–0.98), median specificity was 0.77 (range, 0.62–0.92). Evaluating a positive step versus a congruent joint simulating a shortened radius resulted in a median sensitivity of 0.82 (range, 0.71–0.96) and a median specificity of 1.00 (range, 0.94–1.00). The shortened ulna reflecting a negative RUI was detected with a median sensitivity of 0.96 (range, 0.91–1.00) and a median specificity of 0.98 (range, 0.88–1.00). Sensitivity at detecting an RUI of at least 2 mm was 1.00 for all 3 types of RUI investigated (refer to Table 2 for ranges of sensitivity).

Inter- and IntraObserver Agreement

ICC for interobserver agreement in estimating RUI at 1 mm precisely was 0.87 (95% CI 0.80–0.91). Intraobserver repeatability assessed for 1 investigator was high with an ICC of 0.96 (95% CI 0.94–0.97).

DISCUSSION

To our knowledge, this is the 1st study focusing on both positive as well as negative RUI. Therefore, detection of a congruent radioulnar joint was more challenging in this model of RUI because the investigators could misjudge a congruent joint not only as positive but also as negative RUI. This led to an increased number of false-positive results, reducing specificity to 0.77. Simulating the situation in which the investigators had only to choose between a congruent joint and a positive RUI or between a congruent joint and a negative RUI, specificity was 1.00 and 0.98, respectively. Nevertheless, we feel confident that our complex understanding of RUI is closer to the situation encountered clinically with canine elbow dysplasia.[10] Unfortunately, it makes direct comparison with preceding studies, which only considered positive RUI, difficult.[11–13,25]

Overall visual estimation of RUI using 3D image rendering yielded scores comparable with those reported for radiographic and 2D CT assessment of positive RUI.[11–13,20,25] With a median sensitivity of 0.86 for correct identification of any type of incongruent joint most of the modified elbows were identified as noncongruent. But, because of the already mentioned complexity of both positive and negative RUI, a value of 0.77 as the median specificity for correct identification of any congruent elbow is less than we expected. Being of comparable specificity with plain radiographs or 2D CT measurements,[12,13,25] this specificity (0.77) puts about a

Table 2. Sensitivity and Specificity for the 3 Types of Radioulnar Incongruence (RUI) Investigated (n = 64)

	Sensitivity*		
	RUI 1–2 mm	RUI ≥ 2 mm	Specificity*
Incongruent versus congruent joint	0.86 (0.82–0.98)	1.00 (0.92–1.00)	0.77 (0.62–0.92)
Positive RUI versus congruent joint†	0.82 (0.71–0.96)	1.00 (0.86–1.00)	1.00 (0.94–1.00)
Negative RUI versus congruent joint‡	0.96 (0.91–1.00)	1.00 (1.00–1.00)	0.98 (0.88–0.98)

*Expressed as the median of the 3 independent investigators together with their corresponding maximal and minimal values in parentheses.
†Congruent joint defined as any type of RUI different from a positive RUI.
‡Congruent joint defined as any type of RUI different from a negative RUI.

quarter of congruent elbows at risk of an invasive procedure that may not be indicated. As a consequence we conclude that a highly specific method for accurate estimation of RUI in clinical cases of elbow dysplasia still has to be developed, provided that the cited complex understanding of RUI is true.[10]

For diagnosis of isolated positive RUI (short radius scenario), our method proved superior to what has been claimed as the gold standard.[19,20] With a median sensitivity of 0.82, accurate detection of positive RUI was achieved in most affected cases. Reformatted CT images score comparably well[11,13,20,21]; however, with a median specificity of 1.00, semiquantitative estimation of RUI using 3D image rendering is exceptionally accurate, assuring diagnostic safety when applying the technique in clinical practice. Accuracy further improved when analyzing RUI only with respect to a radioulnar step of ≥ 2 mm. With a sensitivity of 1.00, regardless of the type of RUI investigated, estimation of RUI by means of 3D image rendering would allow for definitive diagnosis of pronounced RUI. Such differentiation of mild versus severe RUI could be relevant, as small RUI remains of unknown clinical significance.[13,19]

The only reported method reaching comparable sensitivity (0.94) with good specificity (0.82) is arthroscopy.[13] Arthroscopy offers the advantage of direct observation of cartilage surfaces instead of indirect estimation of joint incongruence as occurs when performing radiographic as well as CT-based measurements. But arthroscopy is invasive, limiting its usefulness as a screening tool.[21] Moreover, arthroscopic estimation of small RUI might be biased in clinical cases of elbow dysplasia because the radioulnar joint space is often obstructed by fragmentation of the lateral cartilage of the MCP, rendering precise appreciation of the radioulnar transition challenging.[13]

With regard to these potential limitations of arthroscopy, seemingly the ultimate gold standard in evaluating elbow incongruence, and especially small RUI, remains gross anatomic dissection of the joint. This assumption is further supported by the fact that every in vitro study aimed at quantifying RUI has been validated by gross anatomic inspection of the radioulnar joint surface at the end of experiments.[11–13,21,25] Being a maximally invasive procedure not applicable to living patients we aimed at replicating gross-anatomic inspection in a noninvasive way. Extension of CT measurements to the third dimension in the form of high quality 3D renderings of the bony surfaces of the radius and ulna provides a copy of the true anatomy at the level of the subchondral bone. This approach gives a highly realistic, unobstructed view of the radioulnar transition at any level of the radioulnar articulation.

We would estimate the expenditure of time needed to create a 3D model of radius and ulna under clinical conditions to be about 30–40 minutes. This is more than would be desirable for routine clinical use, but it would allow for evaluation of RUI in selected cases. Time of data processing could be decreased by developing a program that automatically segments the humerus and subsequently deletes it from the image volume of interest. Manual segmentation is by far the most time consuming process during image processing, but it must be performed accurately, because the quality of the 3D renderings and, therefore, the evaluation of RUI depends on it to a high degree.

We only investigated semiquantitative visual estimation of RUI. As a consequence the precision gained depends on the experience of the investigator in charge. As documented for radiographic estimation of RUI,[12] relevant operator related differences may be expected. This was also true in our study, even though an ICC of 0.87 attests good interobserver agreement. In combination with an ICC of 0.96 for intraobserver repeatability, our method has the potential to be reliable as well as highly repeatable.

Looking at the investigators separately (Table 1), an obviously high precision was reached for investigator 3. Admitting the fact, that a diagnostic tool should work well in the hands of an average investigator and that, therefore, the median values of sensitivity as well as specificity provided in Table 2 are of primary relevance, the question remains how investigator 3 was able to attain such high precision. The most probable explanation relates to the fact that this person performed the experimental simulation of RUI, including generation of the 3D models. During this time and the process of validation of the experimental setup, he had numerous occasions on which he was aware of the RUI present within the 3D models. Therefore, he could be considered an extensively trained investigator.

Because estimation of RUI within the 64 3D models was performed several months after final image processing and the evaluation was performed randomly in a blinded fashion, we feel confident that the high precision was because of increased experience and not because of "recognition" of the different models.[13] In contrast, the other 2 investigators had only the 5 models shown in Fig 2 for training, rendering them beginners in 3D evaluation of RUI. This finding might suggest that after appropriate training, estimation of RUI by means of 3D renderings might reach values with specificity and sensitivity in the middle range of 0.90. Such high precision seems realistic, because 3D renderings of the proximal radius and ulna offer the potential to assess the complex 3D shape of the radioulnar articulation in all details.

Quantitative measurement of RUI on the 3D model of the radioulnar articulation could eliminate significant operator related error, rendering training dispensable. But distinct and reproducible landmarks on the radioulnar joint space would be needed. Any landmark on the

periphery of the joint could be biased in clinical cases, where secondary arthritis especially in the form of osteophytes develops. Additionally, because of the nature of CT acquisition as well as subsequent 3D image processing and display, edges are inadvertently smoothed, increasing difficulty in reliably identifying comparable landmarks. Measurement of relative radioulnar movement as done in this study for evaluation of induced RUI would not be applicable to individual joints of clinical patients. The axis on which movement of the proximal radius in relation to the ulna had been measured is unknown in clinical cases. Furthermore, the proximodistal movement of the radius was measured with respect to the unchanged, presumably congruent joint (A1). Because canine elbow dysplasia is usually bilateral in presentation, clinical cases would not provide this reference.

Because the published in vitro model was extended to negative RUI, re-evaluation of the precision of experimentally induced RUI at the level of the radioulnar joint space was considered necessary. In previous studies, quantification of the induced RUI was based on measurement of radial shortening in the area of the radial osteotomy.[11–13,20,25] Using that approach, 2 potential errors could be introduced into the experimental setup. First, application of the linear sidebar together with the osteotomy of the radius might produce RUI. If this occurs, an artificially incongruent joint would be defined as congruent, leading to false-positive results. Secondly, the amount of radial shortening measured at the osteotomy does not assure the same amount of RUI present within the joint. The 3D analysis of the 3 congruent CT volumes (A1–A3) allowed us to conclude that any state of RUI induced at any later stage of the experiment truly reflected an RUI different from the one seen in sound, unaffected elbows. On the other hand, simulating a congruent joint indeed did result in the same radioulnar conformation as we would have seen in the native, unchanged elbow. The high correlation of presumed RUI and the one measured with respect to the unchanged elbow in the subsequent 3D models of RUI proved that negative as well as positive RUI could experimentally be induced at high precision using this extended in vitro model.

This leads to what we think is the major limitation of our study as well as all other in vitro studies on RUI.[11–13,25] Related to the nature of "good in vitro practice," only joints from mature dogs, free of proven joint pathology, were used. Finally, RUI was produced by axial movement of the radial head with respect to the ulna. That means, that we tried to mimic developmental humeroradioulnar incongruence by axial movement of a well-shaped joint surface within an otherwise physiologically shaped joint. However, this approach completely neglects the fact that joint incongruence in the form of elbow dysplasia is supposed to take place at an early stage of skeletal development, at which bone, cartilage, and periarticular soft tissues are exposed to a daily process of adaptation and remodeling. At that time, the development of the final microanatomic conformation of the apposing joint surfaces does not only depend on genetic predisposition, but more importantly on the mechanical stimulus exerted on the joint as well.[26]

Hamrick stated in his paper on the elaboration of the "chondral modeling theory" originally developed by Frost,[26,27] that "the articular surfaces of a growing joint must, in order for the locomotor system to function effectively, follow a developmental trajectory that maintains both a normal pattern of joint movement and an acceptable stress distribution within the articular cartilage throughout postnatal ontogeny." The general role of mechanical factors in limb joint morphogenesis is also supported by Ogden who stated that "postnatally, joint motion and joint reaction forces are extremely consequential to the final adult joint contours,"[28] Expanding this theory to elbows with any type of incongruence, it seems evident that even in the case of a pure axial RUI, which we do not believe occurs in most cases, the mechanism of adaptive joint modeling will lead to malformation of the whole joint. This theory is illustrated in a series of antebrachial growth deformities in 34 dogs.[29] It was found that apart from an obvious radial length deficit causing severe RUI, malformation of the elbow joint was a common finding, which persisted even after radial lengthening by use of distraction osteogenesis. However, correction of radial length deficit had a more favorable outcome when performed at a young age, indicative for an adaptive mechanism of the adjacent epiphysis counterbalancing already present malformation.

Therefore, we propose looking at elbow incongruence more in terms of 3D shape analysis of the apposing joint surfaces instead of focusing on a type of RUI of probably purely artificial character. The presence of local incongruence at the apex of the MCP without obvious RUI has already been documented,[20] supporting our understanding of elbow incongruence. As for the human elbow joint,[30,31] detailed analysis of the 2D and 3D shape of the humeroradioulnar joint surface as well as estimation of joint contact conditions by contact area analysis may provide the relevant insight into what the British Veterinary Orthopaedic Association has called "the enigmas of the canine elbow."[32]

Experimentally induced positive as well as negative RUI can be identified in vitro at high precision using 3D renderings of the radioulnar joint surface. Measurement of RUI at the level of the subchondral bone may be less prone to bias because of osteoarthritic changes within the joint space and is also noninvasive. Additionally, it may serve as the future basis for more elaborate analysis of joint shape appraising elbow incongruence in a more

physiologic way. However, currently, arthroscopy remains the superior modality for identification of a positive RUI in vitro.

REFERENCES

1. Samoy Y, Van Ryssen B, Gielen I, et al: Review of the literature: elbow incongruity in the dog. Vet Comp Orthop Traumatol 19:1–8, 2006
2. Gemmill TJ, Clements DN: Fragmented coronoid process in the dog: is there a role for incongruency? J Small Anim Pract 48:361–368, 2007
3. Danielson KC, Fitzpatrick N, Muir P, et al: Histomorphometry of fragmented medial coronoid process in dogs: a comparison of affected and normal coronoid processes. Vet Surg 35:501–509, 2006
4. Wind AP: Elbow incongruity and developmental elbow diseases in the dog: part I. J Am Anim Hosp Assoc 22:712–724, 1986
5. Kirberger RM: Elbow dysplasia in the dog: pathophysiology, diagnosis and control. J South Afr Vet Assoc 69:43–54, 1998
6. Olson NC: Asynchronous growth of the canine radius and ulna: surgical correction following experimental premature closure of the distal radial physis. Vet Surg 10:125–131, 1981
7. Olson NC, Carrig CB, Brinker WO: Asynchronous growth of the canine radius and ulna: effects of retardation of longitudinal growth of the radius. Am J Vet Res 40:351–355, 1979
8. Preston CA, Schulz KS, Taylor KT, et al: In vitro experimental study of the effect of radial shortening and ulnar ostectomy on contact patterns in the elbow joint of dogs. Am J Vet Res 62:1548–1556, 2001
9. Meyer-Lindenberg A, Fehr M, Nolte I: Co-existence of ununited anconeal process and fragmented medial coronoid process of the ulna in the dog. J Small Anim Pract 47:61–65, 2006
10. Lozier SM: New prospectives in elbow dysplasia, in 13th ESVOT Congress, Munich, 7–10 September 2006, Munich, Germany, pp 93–96
11. Holsworth IG, Wisner ER, Scherrer WE, et al: Accuracy of computerized tomographic evaluation of canine radioulnar incongruence in vitro. Vet Surg 34:108–113, 2005
12. Mason DR, Schulz KS, Samii VF, et al: Sensitivity of radiographic evaluation of radio-ulnar incongruence in the dog in vitro. Vet Surg 31:125–132, 2002
13. Wagner K, Griffon DJ, Thomas MW, et al: Radiographic, computed tomographic, and arthroscopic evaluation of experimental radio-ulnar incongruence in the dog. Vet Surg 36:691–698, 2007
14. Slocum B, Pfeil I: Radius elongation for pressure relief of the coronoid process of the ulna, in 12th ESVOT Congress, Munich, 10–12 September 2004, Munich, p 259
15. Mason DR, Schulz KS, Fujita Y, et al: Measurement of humeroradial and humeroulnar transarticular joint forces in the canine elbow joint after humeral wedge and humeral slide osteotomies. Vet Surg 37:63–70, 2008
16. Fujita Y, Schulz KS, Mason DR, et al: Effect of humeral osteotomy on joint surface contact in canine elbow joints. Am J Vet Res 64:506–511, 2003
17. Puccio M, Marino DJ, Stefanacci JD, et al: Clinical evaluation and long-term follow-up of dogs having coronoidectomy for elbow incongruity. J Am Anim Hosp Assoc 39:473–478, 2003
18. Ness MG: Treatment of fragmented coronoid process in young dogs by proximal ulnar osteotomy. J Small Anim Pract 39:15–18, 1998
19. Kramer A, Holsworth IG, Wisner ER, et al: Computed tomographic evaluation of canine radioulnar incongruence in vivo. Vet Surg 35:24–29, 2006
20. Gemmill TJ, Mellor DJ, Clements DN, et al: Evaluation of elbow incongruency using reconstructed CT in dogs suffering fragmented coronoid process. J Small Anim Pract 46:327–333, 2005
21. Gemmill TJ, Hammond G, Mellor D, et al: Use of reconstructed computed tomography for the assessment of joint spaces in the canine elbow. J Small Anim Pract 47:66–74, 2006
22. Schroeder W, Martin K, Lorensen B: The Visualization Toolkit. An object-oriented approach to 3D graphics (ed 4). New York, NY, Kitware Inc, 2006
23. Böttcher P, Maierl J, Hecht S, et al: Automatic image registration of three-dimensional images of the head of cats and dogs by use of maximization of mutual information. Am J Vet Res 65:1680–1687, 2004
24. Gottschalk S, Lin MC, Manocha D: OBB-Tree: a hierarchical structure for rapid interference detection, in Proceedings of the 23rd ACM SIGGRAPH, New York, NY, ACM, 1996, pp 171–180
25. Blond L, Dupuis J, Beauregard G, et al: Sensitivity and specificity of radiographic detection of canine elbow incongruence in an in vitro model. Vet Radiol Ultrasound 46:210–216, 2005
26. Hamrick MW: A chondral modeling theory revisited. J Theor Biol 201:201–208, 1999
27. Frost HM: A chondral modeling theory. Calc Tissue Intl 28:181–200, 1979
28. Ogden JA: Chondro-osseous development and growth, in Urist MR (ed): Fundamental and Clinical Bone Physiology. Philadelphia, PA, JB Lippincott, 1980, pp 108–171
29. Theyse LF, Voorhout G, Hazewinkel HA: Prognostic factors in treating antebrachial growth deformities with a lengthening procedure using a circular external skeletal fixation system in dogs. Vet Surg 34:424–435, 2005
30. Lawlor G, Hennessy R, Carr AJ, et al: 3D analysis of elbow joint geometry, in 16th Meeting of the Northern Ireland Biomedical Engineering Society, Sligo, Ireland, 26 and 27 January 2002, p 81
31. Waide DV, Lawlor GJ, McCormack BA, et al: The relationship between surface topography and contact in the elbow joint: development of a two-dimensional geometrical model in the coronal plane. Proc Inst Mech Eng [H] 214:413–423, 2000
32. BVOA: enigmas of the canine elbow, in Autumn Scientific Meeting, November 2006, Chester, England